Environmental Pollution 278 (2021) 116907

Contents lists available at ScienceDirect

Environmental Pollution

journal homepage: www.elsevier.com/locate/envpol

Comparison of the chronic toxicities of graphene and graphene oxide toward adult zebrafish by using biochemical and phenomic approaches☆

Gilbert Audira [a, b, 1], Jiann-Shing Lee [c, 1], Petrus Siregar [a, b, 1], Nemi Malhotra [d], Marri Jmelou M. Rolden [e], Jong-Chin Huang [f], Kelvin H.-C. Chen [f], Hua-Shu Hsu [c], Yuchun Hsu [c], Tzong-Rong Ger [d, g], Chung-Der Hsiao [a, b, g, *]

[a] Department of Chemistry, Chung Yuan Christian University, Chung-Li, 320314, Taiwan
[b] Department of Bioscience Technology, Chung Yuan Christian University, Chung-Li, 320314, Taiwan
[c] Department of Applied Physics, National Pingtung University, Pingtung, 90003, Taiwan
[d] Department of Biomedical Engineering, Chung Yuan Christian University, Chung-Li, 320314, Taiwan
[e] Faculty of Pharmacy and the Graduate School, University of Santo Tomas, Manila, 1008, Philippines
[f] Department of Applied Chemistry, National Pingtung University, Pingtung, 90003, Taiwan
[g] Center for Nanotechnology, Chung Yuan Christian University, Chung-Li, 320314, Taiwan

ARTICLE INFO

Article history:
Received 17 November 2020
Received in revised form
27 February 2021
Accepted 5 March 2021
Available online 10 March 2021

Keywords:
Graphene
Graphene oxide
Danio rerio
Behaviors
Biomarkers

ABSTRACT

Graphene (GR) and graphene oxide (GO) are widely being used as promising candidates for biomedical applications, as well as for bio-sensing, drug delivery, and anticancer therapy. However, their undesirable side effects make it necessary to assess further the toxicity and safety of using these materials. The main objective of the current study was to investigate the toxicities of GR and GO in predicted environmental relevant concentrations in adult zebrafish (*Danio rerio*), particularly on their behaviors, and conducted biochemical assays to elucidate the possible mechanism that underlies their toxicities. Zebrafish was chronically (~14 days) exposed to two different doses of GR (0.1 and 0.5 ppm) or GO (0.1 and 1 ppm). At 14 ± 1 days, a battery of behavioral tests was conducted, followed by enzyme-linked immunosorbent assays (ELISA) test on the following day to inspect the alterations in antioxidant activity, oxidative stress, and neurotransmitters in the treated zebrafish brain. An alteration in predator avoidance behavior was observed in all treated groups, while GR-treated fish exhibited abnormal exploratory behavior. Furthermore, altered locomotor activity was displayed by most of the treated groups, except for the high concentration of the GR group. From the ELISA results, we discovered a high concentration of GR exposure significantly decreased several neurotransmitters and cortisol levels. Meanwhile, elevated reactive oxygen species (ROS) were displayed by the group treated with low and high doses of GR and GO, respectively. These significant changes would possibly affect zebrafish behaviors and might suggest the potential toxicity from GR and GO exposures. To sum up, the present study presented new evidence for the effects of GR and GO in zebrafish behavioral dysregulation. We hope these assessments can contribute to our understanding of graphene and graphene oxide biosafety.

1. Introduction

Graphene (GR), a single-layer hexagonal lattice composed of carbon atoms, is the simplest form of the carbon layer and the thinnest material produced up to now (Novoselov and Geim, 2007). With a typical thickness of 0.34 nm, a single or few-layer GR can be obtained from high-purity graphite using either a chemical or a mechanical approach (Sajibul et al., 2016). It is formed by a sheet of pure carbon atoms bonded by an sp2-hybridized configuration,

☆ This paper has been recommended for acceptance by Sarah Harmon.

* Corresponding authors. Department of Chemistry, Chung Yuan Christian University, Chung-Li, 32023, Taiwan.
E-mail address: cdhsiao@cycu.edu.tw (C.-D. Hsiao).

[1] These authors contributed equally to this work.

https://doi.org/10.1016/j.envpol.2021.116907
0269-7491/

which is the basic structural element of other carbon allotropes, such as charcoal, graphite, fullerenes, and carbon nanotubes (Geim, 2009; Layek and Nandi, 2013). Meanwhile, graphene oxide (GO), another two-dimensional (2D) carbon material, is known as the oxidized form of GR with a carbon layer decorated by oxygen functional-groups as a result of oxidation and chemical exfoliation of layered crystalline graphite (Park and Ruoff, 2009; Stankovich et al., 2007). Although GO is similar to GR, its properties are very different from that of GR. GO nanosheets are hydrophilic in nature due to the presence of the oxygen functional groups. Thus, due to its hydrophilicity, GO is easily dispersed in water, where it breaks up into atomically macroscopic thin flakes and leads to form the suspensions of single-layer GO (Stankovich et al., 2007). However, GO is not dispersive in organic solvents. Meanwhile, GR possesses a hydrophobic conjugated carbon network that makes it easy to be modified by various kind of functional molecules and nanostructures through hydrophobic, π-π stacking, and chemisorption interactions (Yusoff, 2014).

Since it was discovered in 2004, scientists have engaged in research of GR- and GO-based nanomaterials because of their distinct physicochemical properties. The unique structure allows it to have many unusual and attractive properties including large surface area, an unusual quantum hall effect, superior intrinsic electron mobility, and exceptional thermal conductivity (Hu et al., 2017b). These excellent properties make GR and graphene derivatives versatile materials in a broad range of areas, including separation of environmental pollution (Ding et al., 2015; Kim et al., 2016), non-volatile memory devices (Khurana et al., 2014; Kim et al., 2016), energy storage devices (Mendoza-Sánchez and Gogotsi, 2016), optical instruments (Gao et al., 2015), sensors (Furue et al., 2017), catalysis (Hu et al., 2017a; Paredes and Villar-Rodil, 2016), and as a surfactant with some overlaps between these fields. However, so far as the nanomedicine applications are concerned, GR and GO's potential toxicity has received relatively little attention (Perrozzi et al., 2014) while toxicity is an important issue that must be addressed to regulate their usage related to living matters.

Several studies reported the toxicities of GR and GO in various animal models. In a rat study, one dose of PEG-nGO (5 mg/kg) was exposed to female albino rats. The results showed increased malondialdehyde (MDA), a lipid peroxide, concentration and reduction in the activity levels of antioxidants enzymes which indicated oxidative stress in all organs of the injected organisms (Ain et al., 2019). In zebrafish (*Danio rerio*), acute exposure of GR was found to modulate the antioxidant system in *D. rerio* with brain and gills as its primary target organs (Fernandes et al., 2018). In another prior study, adult zebrafish were acutely and chronically exposed to GO at a concentration 2, 10, and 20 mg/L. Later, necrotic and apoptotic stages in zebrafish gill cells with a generation of ROS after 24 h of exposure were demonstrated while significant alteration of liver and gills tissue was observed after 2 weeks of chronic exposure. Afterward, they concluded the organ-specific effects of GO and the assumption of the long-term effect on fish due to GO presence in the aquatic environment (Souza et al., 2017). The summary of GR and GO's biological effects in animals from previous studies can be found in Table S1.

Zebrafish has emerged not only as a powerful vertebrate model for aquatic toxicology. In nanomaterial studies, it also has been established as an important preclinical model for *in vivo* toxicity studies of nanomaterials. (Sawle et al., 2010). Not only due to its sensitivity to pollutants, but its close homology with the human genome and ease of maintenance also make zebrafish a suitable model organism to be used in the current *in vivo* study to evaluate GR and GO toxicities in aquatic environments (Malhotra et al., 2020b; Seabra et al., 2014; Souza et al., 2017). However, even though GR and GO toxicities have been addressed in some prior studies, little is still known about their effects on adult zebrafish behavior. Moreover, most of the studies in adult zebrafish or more sentient animals used relatively higher concentrations than the predicted environmental concentration (Yang et al., 2019). Based on this consideration, the specific objective of this study was to investigate and compare GR and GO's potential adverse effects at predicted environmental relevant concentrations in adult zebrafish, particularly on their behaviors, since nowadays, behavioral assessment has emerged as a crucial tool to inspect toxicology of materials. In fact, a prior study showed that neurobehavioral study gave more relevant and reliable results, aside from its less cost, robustness, and effectiveness for toxicology research (Audira et al., 2020b; Kalueff et al., 2016). Also, to further examine their effects under different concentrations, two doses of GR and GO were studied. Furthermore, biochemical assays were conducted to elucidate the possible mechanism that underlies their behavior toxicities. The current study's hypothesis was that chronic exposure of both GR and GO, even in predicted environmental concentrations, would affect zebrafish behavior. The overview of the experimental design of the current study is shown in Fig. S1.

2. Methods

2.1. Physical properties characterization of graphene-based nanomaterials

In order to acquire the unique bulk and surface structure of the graphene-based materials, some characterization techniques were used in the study, including Raman spectroscopy, X-ray diffraction (XRD), transmission electron microscopy (TEM), atomic force microscopy (AFM), and ultraviolet–visible spectroscopy (UV–vis). Single-layer GR and GO were purchased as a 100 ml aqueous suspension with 2 mg/ml of solid GR and 1 mg/ml of solid GO contents from Tanfeng Tech. Inc. (Jiangsu, China).

XRD peak positions are used to reveal the crystalline phase and interplanar distance (*d*-spacing) for both test samples, GR and GO. A few drops of these two different dispersions were vacuum-dried on a silicon substrate to carry out the XRD analysis. Afterward, by using a Bruker D8 Advanced eco (Billerica, MA, USA) with a CuKα radiation source, their X-ray diffraction patterns were acquired. The scanning condition for this analysis was an angular range of 5°-80° (2θ), a 0.02° step size, and 1.2 s per step.

Raman spectra were measured using a microscopic Raman system (RAMaker, Protrustech Co., Ltd., Taiwan). The excitation wavelength was 532 nm. The scanned spectral range was 1000–3000 cm^{-1} with a spectral resolution of 1 cm^{-1} and accumulation times were typically six collections of 90 s with six scans per spectrum. Furthermore, as a reference for calibration (520 cm^{-1}), a silicon standard sample was used. The samples were prepared by dripping a small quantity of each aqueous solution on a silicon substrate. Raman spectra of air-dried samples were collected at random points under a 20 × objective. In addition, to detect the conjugation network and absorption of GR and GO, absorbance from 200 to 800 nm was monitored automatically in each material through Jasco V-770 double beam spectrophotometer (Jasco Co., Japan).

The only technique that can be used to observe particle size distribution for GR-based materials directly is microscopy. Therefore, the surface morphology, including shape, morphology, and size of these two test compounds was examined by Transmission Electron Microscopy (TEM) images. TEM analyses were carried out using a Hitachi H-7500 TEM (Hitachi, Tokyo, Japan), operating in TEM mode at 80 kV. TEM samples were prepared by dropping

about 0.1 mL of diluted dispersion on Cu grids with a carbon film. The size distributions of these two samples were obtained by measuring 100 nanoparticles, using AMT image capture software.

Atomic Force Microscopy (AFM) measurements of both samples were performed under ambient conditions using an AFM (SPA400, *SII* nanotechnology, Co., Ltd, Japan) in the intermittent-contact (tapping) mode (120 kHz) with a sharp Si-tip cantilever (7 nm). All samples were prepared by drop-casting using a mica substrate and were dried in a vacuum chamber. The lateral dimension and height distribution of these materials were determined by analyzing AFM images using NanoNavi-SPA400 (Minato-ku, Tokyo, Japan) software. Images were acquired at a resolution of 256 pixels and 256 lines and at a scan rate of 1 Hz. In addition, the nominal spring constant of the cantilevers was 13 Nm^{-1}. Furthermore, to study the stability of colloidal dispersions, the zeta potential of these two GR-based materials was measured using an SZ-100 dynamic light scattering system (Horiba, Kyoto, Japan). Zeta potential was measured at 25 °C after the suspension was homogenized by high-intensity ultrasonic waves for 15 min.

2.2. Animal ethics and zebrafish husbandry

All experimental procedures and protocols were authorized by Committee for Animal Experimentation of Chung Yuan Christian University Committee (CYCU109001, Jan. 2, 2020). All animal tests were carried out following the regulations released by CYCU's Institutional Animal Care and Use Committees (IACUCs). In the present study, we used healthy AB strain zebrafish (6–7 months) with mixed genders. Prior to the GR or GO exposure, adult zebrafish were reared in a zebrafish facility with a 14/10 h light/dark cycles and temperature of 26 ± 1 °C, and were fed with either brine shrimps or commercial dry food twice a day (Aleström et al., 2019; Lawrence, 2007). Zebrafish were kept in circulating UV sterilized water with 0.254 ± 0.004 mS/cm of electrical conductivity, 6.5 ± 0.2 mg/L of dissolved oxygen, 183 ± 5 mg of $CaCO_3$/L for water hardness, and pH 7.2 + 0.4. In addition, to filter the circulating water, reverse osmosis was used. Zebrafish routine culture and maintenance were according to the prior publication (Avdesh et al., 2012).

2.3. Exposure of graphene and graphene oxide

Two doses of GR (0.1 and 0.5 ppm) and GO (0.1 and 1 ppm) were prepared before use. Since information regarding the environmental concentration of GO or concentration of GR-family nanomaterials (GFNs) in natural waters are not yet reported, the determination of concentration applied in the current study was based on the predicted environmental concentration of GO in the water system, which is around 0.001–1 mg/L (Goodwin et al., 2018; Nouara et al., 2013; Yang et al., 2019). In addition, the determination of the GO concentrations was also considering prior studies in zebrafish embryos that found 10 ppm of GO was a no-observed-effect concentration (NOEC) while developmental toxicities in zebrafish larvae were induced by 1–100 μg/L GO (Markovic et al., 2018; Zhang et al., 2017). Furthermore, the comparable concentrations of GR to GO were chosen since there was no study of the GR's effect in adult zebrafish that can be used as the reference, except a prior experiment by Fernandes et al. that injected intraperitoneally high concentrations (5 and 50 mg/L) of graphene in adult zebrafish (Fernandes et al., 2018). Unfortunately, these concentrations could not be applied in the current study because we found a high mortality rate in the 1 ppm GR-treated group during the incubation period which also explains the usage of 0.5 ppm GR instead of 1 ppm. Moreover, in order to achieve the objective of this study, these concentrations were chosen to provide more direct and valid comparisons of GR and GO. Afterward, zebrafish were randomly divided into five groups with ~20 adult zebrafish for each group. To avoid experimental bias, a simple random allocation method was used (Audira et al., 2020a). The current sample size was determined by a statistical power analysis in all groups. Based on the analysis, to achieve a confidence interval of 90% and 9 units of a margin of error, a 22 size number was required. Moreover, the sample size applied in other prior adult zebrafish behavior studies also became our consideration regarding the sample size determination (de Abreu and Giacomini, 2019; Kolesnikova et al., 2019; Volgin et al., 2019). Later, all groups were incubated in a 4 L tank water with 0 (control), 0.1 ppm GR, 0.5 ppm GR, 0.1 ppm GO, and 1 ppm GO for ~14 days in 5 L glass tanks. The continuous aeration was applied in the glass tanks during the entire experiment period to maintain the particles' dispersion in the test solution. The tested fish were fed with either brine shrimps or commercial dry food twice a day. In addition, the water in each tank was completely renewed every 48 h during the chronic treatment, and the stock solution of either GR or GO was added to the final concentration to maintain the constant concentration of these materials. This renewal of exposure medium protocol was carried out based on several previous studies in GO and other materials (Jia et al., 2019a; Ni et al., 2019; Qiang et al., 2016; Souza et al., 2018). Moreover, this procedure was also important to prevent any possibility of bacterial infection caused by bad water quality, which might come from excess foods after feeding.

2.4. Adult zebrafish behavior tests

After the fish were incubated in the predetermined time, zebrafish behavioral tests as in the order of novel tank exploration, shoaling, mirror biting, conspecific social interaction, and predator avoidance behavior tests, which were according to the prior publication, were carried out in all five groups (Audira et al., 2018). The behavior tests were performed in a test room with 26 ± 1 °C temperature within the morning until the afternoon (10:00 to 16:00). In avoiding stress condition in the tested fish, all the behavior tests were divided into three sessions and carried out on three consecutive days. Novel tank exploration and shoaling tests were conducted on the thirteen-day exposure. Novel tank exploration test was conducted as the first behavior test since the tested fish had not been introduced to the test tank previously, thus, their behavioral responses toward the novel environment would be more genuine and reliable. Meanwhile, on the following day, the experiment was continued with mirror biting and conspecific social interaction tests. Finally, on fifteen days of exposure, predator avoidance behavior test was performed. This behavior test was preferred to be conducted as the last behavior test because, in this test, the convict cichlid (*Amatitlania nigrofasciata*) was supposed to induce the fear response on the tested fish and since fear can be possessed by the fish for some period, it could affect their behavior in the following behavior tests. A trapezoid plastic tank, with dimensions: 15.9 cm along the diagonal side, 22 cm bottom, and 15.2 cm high was used for all behavioral tests. ~1.25 L of filtered water was filled to each tank. Before the tests, 3–5 min of acclimation in the test tank was applied to all tested fishes, except for the novel tank test since in this test, fish behavioral response to a new environment was recorded as soon as the tested fishes were placed in the test tank for 1 min every 5 min interval for 31 min. For the mirror biting tests, on one side of the tank wall, a mirror was inserted to form a fish reflection as a stimulus to measure the fish's aggressiveness level. Meanwhile, a transparent glass separator was placed inside the tank in the predator avoidance behavior and conspecific social interaction tests. This transparent separator was

used to separate test fish either with *A. nigrofasciata* in the predator avoidance test or another zebrafish as its conspecific in the conspecific social interaction test. Lastly, a shoaling test with three fish as the shoal size was performed in the tank without any modification. After acclimation, zebrafish behavior response to a specific stimulus in each of these four behavior tests was recorded for 5 min. Fish behavior was recorded with Canon EOS 600D digital single-lens reflex camera with a 55–250 mm lens (Canon Inc., Tokyo, Japan). Each assay was performed in two replicates per treatment with 11 fish per replicate ($n = 22$). Afterward, idTracker, a movement tracking software, was utilized to track zebrafish activity and movement from the videos based on the prior study (Pérez-Escudero et al., 2014). Afterward, several critical endpoints in each behavioral test were calculated (Audira et al., 2018). Trained observers blinded to the treatments were selected to process all zebrafish behaviors.

2.5. Tissue preparation and total protein determination

After behavior tests, immediate anesthetization and euthanization were performed on the zebrafish by immersed them in tricaine (A5040, Sigma, St. Louis, MO, USA). Later, its whole brain tissues were extracted for subsequent biochemical analyses. A single homogenate for each sample, which consisted of four to five whole zebrafish brains, was prepared. Subsequently, in volumes of 10 (v/w) of ice-cold phosphate-buffered saline (PBS), the homogenate was standardized at pH 7.2. Next, a tissue homogenization was performed by using a bullet blender (Next Advance, Inc., Troy, NY, USA), followed by centrifugation at 13,000 rpm for 15 min. Afterward, we kept the supernatant in micro Eppendorf tubes, and for the following experiment; it was stored in the freezer at −20 °C. Pierce BCA Protein Assay Kit (23,225, Thermo Fisher Scientific, Massachusetts, MA, USA) was used to determine the total protein concentration in brain tissues. Subsequently, by using a microplate reader, we analyzed the color formation at 562 nm (Multiskan GO, Thermo Fisher Scientific, Waltham, MA, USA).

2.6. Quantification of stress hormones, oxidative stress markers, and neurotransmitters in zebrafish brain tissues

Zebrafish brain tissues were analyzed to determine GR and GO exposures' possible effects in influencing oxidative stress, antioxidant activity, and neurotransmitter changes in the zebrafish brain. Reactive oxygen species (ROS), a tissue oxidative stress marker, was measured by ELISA kits (ZGB-E1561). Meanwhile, cortisol, as one of the stress hormones, was also quantified by using commercial ELISA kits (ZGB-E1575). Lastly, neurotoxic response biomarkers, including serotonin (5-HT, ZGB-E1572), acetylcholine (ACh, ZGB-E1585), kisspeptin (KISS, ZGB-E1696), dopamine (DA, ZGB-E1573), acetylcholine esterase (AChE, ZGB-E1637), and oxytocin (OT, ZGB-E1668) were also measured by target-specific ELISA kits. All ELISA kits were acquired from Zgenebio Inc. In Taipei, Taiwan. Afterward, by using a microplate reader, we analyzed the absorbance at 450 nm (Multiskan GO, Thermo Fisher Scientific, Waltham, MA, USA). The total protein relative concentration was measured according to the standard curve provided by the kits. All quantifications were carried out in accordance with the manufacturing protocols. Five biological replicates were applied in the analysis.

2.7. Statistical analyses

In the novel tank test, we used two-way ANOVA with Geisser-Greenhouse correction continued with Dunnett's multiple comparisons test to calculate the significant differences between the treated and untreated groups during the whole 30 min test. Meanwhile, for other behavioral tests, normality tests, including Kolmogorov-Smirnov, Shapiro-Wilk, D'Agostino & Pearson, and Anderson-Darling tests, were carried out beforehand to test the normality of data distribution. If the data passed all of the normality tests, one-way ANOVA continued with Dunnett's multiple comparisons test was used. On the other hand, if the data did not pass in all normality tests, Kruskal-Wallis followed with Dunn's multiple comparisons test, a nonparametric test, was applied since the assumption of normal distribution did not require by this analysis (Adams and Anthony, 1996). The behavioral data are displayed as median with interquartile range. We chose median to express the data since generally, it is used to describe data in a skewed distribution, such as behavior data (Privitera, 2015; Salkind, 2009). Similar to behavioral tests, normality tests were also conducted in biochemical data before the statistical test. Since all biochemical data passed both Shapiro-Wilk and Kolmogorov-Smirnov tests, Brown-Forsythe and Welch ANOVA test with Dunnett's T3 multiple comparisons test, a parametric test, was used. For all data analyses, both GR-treated groups and GO-treated groups were compared to the control group separately. The biochemical data are displayed as mean with a standard deviation (SD). GraphPad Prism (GraphPad Software version 8 Inc., La Jolla, CA, USA) was used to analyze and plot all data, except for the novel tank test. The violin plot was used for most of the behavioral data since it is better than box plot to observe the distribution of the data, which was not normally distributed in the current study (Kuhn and Johnson, 2019). For the novel tank test results, we used Origin® 2019b (Origin® Software version 2019b Inc., Northampton, MA, USA) to generate the radar plot. Radar plot was used to simplify the results and is one of the common plots used to represent the animal behavioral data (Buenafe et al., 2013; Orellana-Paucar et al., 2013; Steele et al., 2018). Asterisks of *, * *, * * *, or * * * * were used to mark the significant differences between treated and untreated groups if p-value < 0.05, <0.01, <0.001, or <0.0001, respectively. All of the statistical analyses were conducted by blind-trained analysts.

2.8. Clustering, heatmap, and PCA analysis

After the value differences between the treated and untreated groups in each behavior test were calculated, they were loaded to Microsoft Excel and input into an excel file. The list and description of all behavioral endpoints were listed in Table S2, as discussed in the prior study (Audira et al., 2018). The behavioral data of other treatment groups, including C-60 NPs, C-70 NPs, Fe_3O_4 MNPs, and C-MNP, were obtained from previous studies (Malhotra et al., 2019, 2020a; Sarasamma et al., 2018, 2019). Later, after converted to a .csv type file, the file was transferred to ClustVis (https://biit.cs.ut.ee/clustvis/). This web tool is designed to visualize and cluster multivariate data. In addition, for managing every variable equally, unit variance scaling was applied. In calculating the principal components, SVD with the imputation method was used as we did not find any missing value in the dataset (Metsalu and Vilo, 2015). Finally, the principal component analysis (PCA) and heatmap clustering results were copied to the computer.

3. Results

3.1. Physical properties characterization of graphene and graphene oxide nanomaterials

Fig. 1A shows the GR sample did not exhibit a discernible diffraction peak of characteristic (002) plane (about $2\theta = 26^{\circ}$), indicating that the number of GR layers is less than 3 (Huh, 2014). In the XRD pattern of GO, the characteristic peak at $2\theta = 11.1^{\circ}$ was

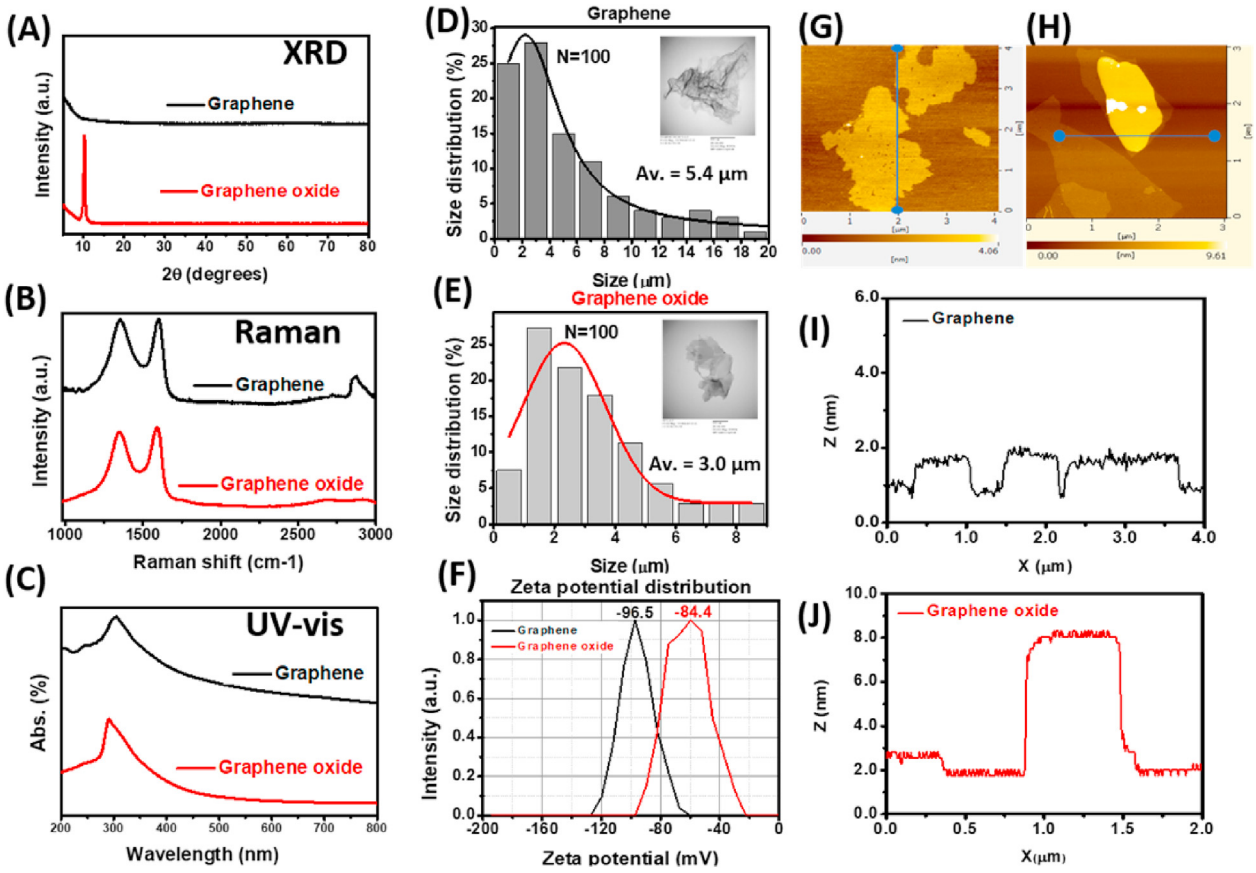

Fig. 1. Physical properties of graphene and graphene oxide used in this study. (A) X-ray Diffraction (XRD) spectrum comparison between graphene (GR, black color) and graphene oxide (GO, red color). (B) Comparison of Raman spectrum between GR (black color) and GO (red color). (C) The UV–visible spectrum between GR (black color) and GO (red color) nanoparticle solutions. Size distribution and transmission electron microscope images of (D) GR and (E) GO nanoparticles. (F) Zeta potentials of GR (black color) and GO (red color) nanoparticle solutions. AFM (atomic force microscope) images of (G) GR and (H) GO. The corresponding height profiles of (I) GR and (J) GO. (For interpretation of the references to color in this figure legend, the reader is referred to the Web version of this article.)

observed, attributed to the diffraction of the (001) crystallographic plane. The corresponding d-spacing was 8.0 Å, which is typical for GO (Geim, 2009). Therefore, it was found that the *d*-spacing value in Graphite Oxide was efficiently higher than that in graphite, which is accounted for the uptake of oxygen-containing functional groups and water molecules between the hydrophilic interlayer basal planes of GO (Chen et al., 2011; Park and Ruoff, 2009).

Raman spectroscopy is a well-known and widespread technique for the analysis of GR and its derivatives. The G peak (at 1580–1605 cm^{-1}) and D peak (at 1320–1350 cm^{-1}) are the two predominant features of the Raman spectrum for GR (Novoselov and Geim, 2007; Sajibul et al., 2016). The sharp and robust G band is visible, while the D band is hardly observed in the highly crystalline graphite (Wei et al., 2013). The D band associated with the edge distortion is considered as an indication of structural disorder. Hence, the intensity ratio of these two bands (I_D/I_G) can indicate the GR-based products' quality. Two additional Raman peaks may also be observed: 2D peak (at 2640–2705 cm^{-1}) and S3 (around 2900 cm^{-1}) peak. The G and 2D bands represent the two-dimensional hexagonal lattice, while the S3 band (~2900 cm^{-1}) is regarded as a second-order peak derived from the D-G peak combination (Hu et al., 2017b; Johra et al., 2014). The intensity ratio of S3 relative to 2D is observed to be proportional to the reduction in defects (Geim, 2009). The I_{S3}/I_{2D} value can be utilized to estimate the content of defects in these two samples. Further, a Raman normalization procedure based on a silicon substrate has been established as a reliable technique to determine the number of layers in GO (Kostiuk et al., 2016). To estimate the layer number of GO, the total integral intensity of G and D bands to that of the second-order optical phonon peak of the silicon substrate (I_{D+G}/I_{Si}) was performed in the study. As shown in Fig. 1B, two characteristic Raman peaks around 1350 cm^{-1} and 1580 cm^{-1} appeared for both samples. The positions of G and D bands of the GO band are almost identical to those of GR. The D band to G band intensity (I_D/I_G) was estimated to be 1.2 in the GO sample case. On the other hand, the GR sample shows a much higher I_D/I_G ratio (1.9), implying a larger number of chemical and structural defects on both edges and basal planes due to the reduction procedure (Munz et al., 2015). A higher intensity ratio (I_{S3}/I_{2D}) was also found in the case of GR compared to that of GO. These experimental results demonstrate that the existence of a higher defect in the GR sample. In addition, the number of layers was estimated to be less than 4 for the GO-based on the measured I_{D+G}/I_{Si} value.

Single-layer GR has zero bandgap, while multilayer GR with an absorbance peak at 230–236 nm will be recorded in the UV–vis spectrum due to π to π^* transition of C=C bonds. On the other hand, GO will exhibit the characteristic n $\rightarrow$ π^* transitions of carbonyl groups (C=O) and $\pi \rightarrow \pi^*$ transitions of aromatic C=C bonds in terms of an absorption band at 230 nm and a shoulder around 300 nm, respectively (Layek and Nandi, 2013). It is worthy to notice in Fig. 1C that a characteristic absorption peak at ~230 nm in these two solutions was shifted to longer wavelengths (~290 for GO and 305 nm for GR), suggesting an extended π-stacking interlayer conjugation (Hu et al., 2017b). Such a shift could be ascribed to

the restoring of electronic conjugation of the C=C bonds within GR sheets and structural ordering after the chemical reduction of GO (Kim et al., 2016). Both samples also show a small absorption peak near 320 nm in the UV–vis spectrum, caused by n-π* electron transition of the C=O bond.

The main driving force of van der Waals interactions makes single-layer GR vulnerable to self-folding, due to the exceptionally low bending stiffness of single-layer GRs (Ding et al., 2015). Accordingly, TEM observations indicated that there are only a few layers thick in the GR sample, in which transparent, folded nanosheets were usually observed (Fig. 1D). By contrast, some dark areas can be seen in GO's TEM image due to the ordered stacking of a few numbers of layers (Fig. 1E). The particle distribution and average size of these two samples were shown in Fig. 1D&E, which indicates a bigger mean particle size of GR (5.4 μm) in comparison with the GO (3.0 μm). Furthermore, in the case of zeta potential, our measurements showed that the mean values of the GR and GO are −96.5 and −84.4 mV, respectively. Zeta potential (ζ) was utilized to study the stability of colloidal dispersions. Generally, because of significant charge repulsions between the layers, particles are considered stable if their zeta potentials are more positive than +30 mV and more negative than −30 mV (Stankovich et al., 2007). Thus, the results suggest the high stability of both dispersions (Fig. 1F).

In addition, to perform the horizontal dimension observation, AFM is regarded as a convenient approach for thickness measurement and layer number counting (Yao et al., 2017). The height profile in the AFM figure corresponds to the height difference between the two points in the figure, the thickness of the GR-based materials. Considering the thickness of single-layer GR, which was 0.34 nm, the layers could be counted. The typical AFM images of GR and GO on the mica surface are shown in Fig. 1G&H. As clearly outlined, GR sheets' thickness in the GR sample was found to be mainly in the size range of 0.4–1.1 nm (Fig. 1I), which is a typical thickness of single- or double-layer GR. After oxidation, the thickness of single-layer GO is generally about 0.7–1.0 nm (Lai et al., 2012; Pan and Aksay, 2011). The GO's layer number is estimated to be 3 or 4 because the low average thickness (2.8 nm) of nanosheets was often observed under AFM (Fig. 1H & J).

3.2. Graphene and graphene oxide effect in locomotion and exploratory behavior test

A novel tank test is a method to observe zebrafish locomotor activity and spatial exploration ability to respond to a novel environment. Here, to observe the changes in their locomotor activity, several behavior endpoints namely average speed, freezing, swimming, and rapid movement time ratios were measured. Meanwhile, to assess the exploratory behavior changes, time in top duration, number of entries to the top, latency to enter the top, total distance traveled in the top, and thigmotaxis were calculated. The detailed information regarding these behavioral endpoints can be found in Table S2. In Fig. 2, we divided the results into two radar plots to display the effects of these materials before and after fish's acclimation since generally, a very clear fish habituation behavior to novelty occurs after ~10 min of novel environment exposure (Wong et al., 2010). After GR and GO exposure, we found a low concentration of GR and GO significantly decreased zebrafish locomotor activity (Fig. 2A&B). However, the locomotion alterations displayed by those groups were shown with different magnitude. The most pronounced hypoactivity was exhibited by 1 ppm GO-treated group, which was indicated by significantly low levels of average speed ($p = 0.0009$; $F(2, 57) = 1.671$) and rapid movement ratio ($p < 0.0001$; $F(2, 57) = 2.857$) and significantly elevated level of swimming time movement ratio ($p < 0.0001$; $F(2, 57) = 3.631$) (Fig. 2C). Following this group, a slightly less robust alteration in the locomotor activity was presented by a 0.1 ppm GR-treated group. Similar to the GO group's high concentration, the same three behavior endpoints were also significantly different from those in the untreated group. However, the significance levels were less than the high concentration of the GO group (Fig. 2C). Lastly, the least pronounced hypoactivity was displayed by the 0.1 ppm GO-treated group. Only two locomotor activity-related endpoints were altered during the test: average speed ($p = 0.0215$; $F(2, 57) = 1.671$) and rapid movement ratio ($p = 0.0148$; $F(2, 57) = 2.857$) (Fig. 2C). Interestingly, there was a tendency of hyperactivity behavior possessed by 0.5 ppm GR-treated group after 11 min of novel tank exposure, even though it did not reach a statistically significant level. Furthermore, both GR groups caused an altered exploratory behavior shown by a significantly low thigmotaxis level ($p < 0.0001$; $F(2, 57) = 8.470$). On the other hand, both GO-treated groups did not show any abnormality in their exploratory behavior (Fig. 2C).

3.3. Graphene and graphene oxide effect in aggressiveness and predator avoidance tests

A mirror biting test was conducted to assess zebrafish's aggressiveness after two weeks of waterborne GR and GO exposure. Generally, zebrafish bites the mirror when it sees its reflection. This phenomenon also indicates social motivation or its intention to communicate with a social partner. No significant alteration in aggressiveness level was found in either GR- or GO-treated fish from the results. This phenomenon is indicated by the similar level of mirror biting time percentage and most prolonged duration in the mirror side between control and both treated groups (Fig. 3A&B). Meanwhile, different results were obtained from the predator avoidance test. Typically, fish shows high anxiety of even freezing behavior as their innate response when facing their natural predator (Ahmed et al., 2011). Predator avoidance test showed that zebrafish chronically treated with both GR and GO possessed less predator avoidance behavior. Similar to locomotor activity results, the severity of alteration was different among the groups. The most pronounced altered predator avoidance behavior was displayed by 0.5 ppm GR-treated group, indicated by a significantly elevated level of approaching predator time ($p < 0.0001$) and significantly low average distance to the predator's separator ($p = 0.0059$) (Fig. 3C&D). Identical with this result, both GO groups also showed alterations in both endpoints, except that their differences to the control group were less significant than 0.5 ppm GR-treated group. Finally, the least altered predator avoidance behavior was exhibited by 0.1 ppm GR-treated group since only one endpoint was significantly different from the control ($p = 0.0321$) (Fig. 3C&D). In addition, in line with the novel tank test result, a hyperactivity-like behavior that displayed by a significantly low level of freezing time movement ratio ($p = 0.0011$) and elevated level of average speed ($p = 0.0015$) and swimming movement time ($p = 0.0042$) was observed in 0.5 ppm GR group (Figs. S2A–C). This phenomenon may indicate that a relatively low concentration of GR alters zebrafish locomotor activity.

3.4. Graphene and graphene oxide effect in social tests

Next, since zebrafish is a highly social animal, conspecific interaction, as one of zebrafish social natures, was assessed by performing social interaction tests (Moretz et al., 2007). Here, the effect of GR and GO on zebrafish social nature was inspected. The results showed that there was no significant alteration between control and treated groups regarding their social interaction. This phenomenon was supported by no significant changes found in all

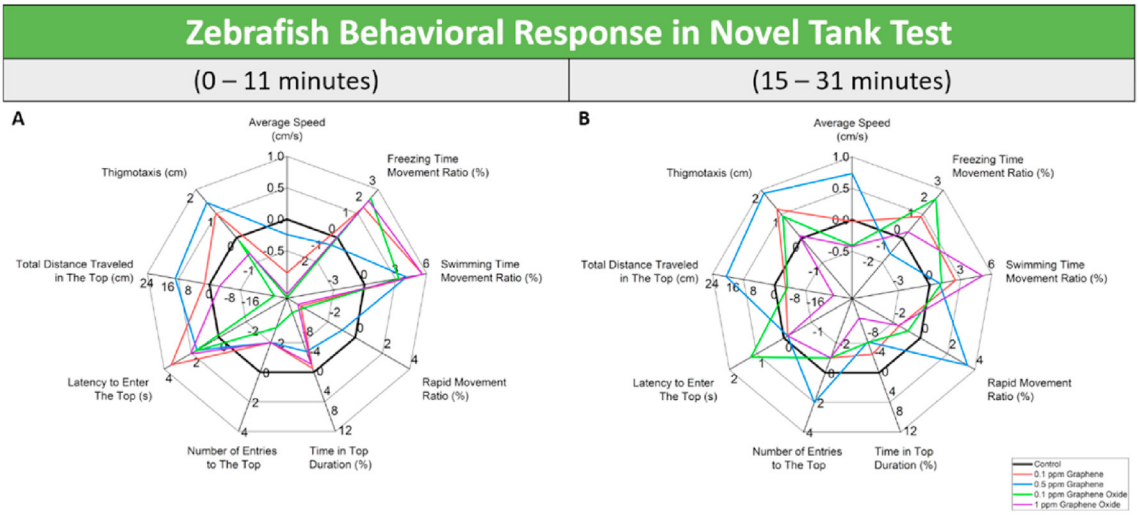

C	Behavior Endpoints	0.1 ppm Graphene	0.5 ppm Graphene	0.1 ppm Graphene Oxide	1 ppm Graphene Oxide
Locomotor Activity	Average Speed (cm/s)	↓* $p = 0.0248$	n.s. $p = 0.4943$	↓* $p = 0.0215$	↓*** $p = 0.0009$
	Freezing Time Movement Ratio (%)	n.s. $p = 0.8437$	n.s. $p = 0.0741$	n.s. $p = 0.6880$	n.s. $p = 0.2355$
	Swimming Time Movement Ratio (%)	↑* $p = 0.0268$	n.s. $p = 0.0886$	n.s. $p = 0.7287$	↑**** $p < 0.0001$
	Rapid Movement Ratio (%)	↓** $p = 0.0015$	n.s. $p = 0.9612$	↓* $p = 0.0148$	↓**** $p < 0.0001$
Exploratory Behavior	Time in Top Duration (%)	n.s. $p = 0.9824$	n.s. $p = 0.6656$	n.s. $p = 0.1214$	n.s. $p = 0.3465$
	Number of Entries to The Top	n.s. $p = 0.0775$	n.s. $p = 0.7387$	n.s. $p = 0.0695$	n.s. $p = 0.0773$
	Latency to Enter The Top (s)	n.s. $p = 0.9110$	n.s. $p = 0.9922$	n.s. $p = 0.0954$	n.s. $p = 0.9161$
	Total Distance Traveled in The Top (cm)	n.s. $p = 0.9445$	n.s. $p = 0.3022$	n.s. $p = 0.2801$	n.s. $p = 0.2010$
	Thigmotaxis (cm)	↓**** $p < 0.0001$	↓**** $p < 0.0001$	n.s. $p = 0.1135$	n.s. $p = 0.8353$

Fig. 2. Profile plots of untreated, graphene, and graphene oxide-treated zebrafish group behavioral responses in the novel tank test (A) before and (B) after 11 min exposure to a novel environment. Two-Way ANOVA with the Geisser-Greenhouse correction was used to analyze the fish swimming activities for 31 min test with a 1-min video every 5 min time interval. The plots are expressed as the differences between median. (C) Summary table of behavioral differences between untreated and treated zebrafish groups. ↓ represents a significant decrease in the value and ↑ indicates a significant increase in the value of comparison between untreated and treated zebrafish groups. Statistical significances were labeled as * $p < 0.05$, ** $p < 0.01$, and **** $p < 0.0001$ while n.s. = not significant ($n = 20$ for all groups).

GR- or GO-treated groups compared to the control (Figs. S3A–C). Later, another social-related assay in form of the shoaling test was conducted to further support the result regarding the effect of these materials in zebrafish social behaviors. As an innate behavior to avoid predators and reduce anxiety, it reflects the complex interaction of fishes swimming together coordinately (Pavlov and Kasumyan, 2000; Shaw, 1960; Wang et al., 2016). In line with the social interaction test, normal shoaling behavior was displayed by all treated fishes, indicated by the same levels of all behavioral endpoints. This endpoint includes the average inter-fish distance, average shoal area, average nearest neighbor distance, and average farthest neighbor distance between control and treated groups (Figs. S3D–F).

3.5. Biochemical assay of biomarkers expression in the brain

To help elucidate the behavioral alterations observed in previous behavioral tests, the effects of chronic exposure to GR and GO on selected neurotransmitters, antioxidant activity, and oxidative stress in zebrafish brains were investigated. First, we measured the neurotransmitter levels and found several neurotransmitters, which were serotonin, acetylcholine, and dopamine, were significantly decreased in brain tissue in 0.5 ppm GR-exposed fish (Table 1). However, this phenomenon was not observed in other treatment groups. Furthermore, normal levels of kisspeptin, acetylcholinesterase, and oxytocin were shown in the brain tissue of either GR- or GO-treated groups. Like the neurotransmitter results, chronic exposure of 0.5 ppm GR caused a significant reduction of cortisol in adult zebrafish. On the other hand, intriguing results were found during reactive oxygen species (ROS) measurements. From the result, a significantly high level of ROS was displayed in both 0.1 ppm GR- and 1 ppm GO-treated groups.

3.6. Phenomics of graphene and graphene oxide toxicities

Next, to investigate the difference in terms of behavioral alteration patterns between GR, GO, and other nanoparticle chemical toxicities, a phenomics approach was used. Thus, C-60 NPs, C-

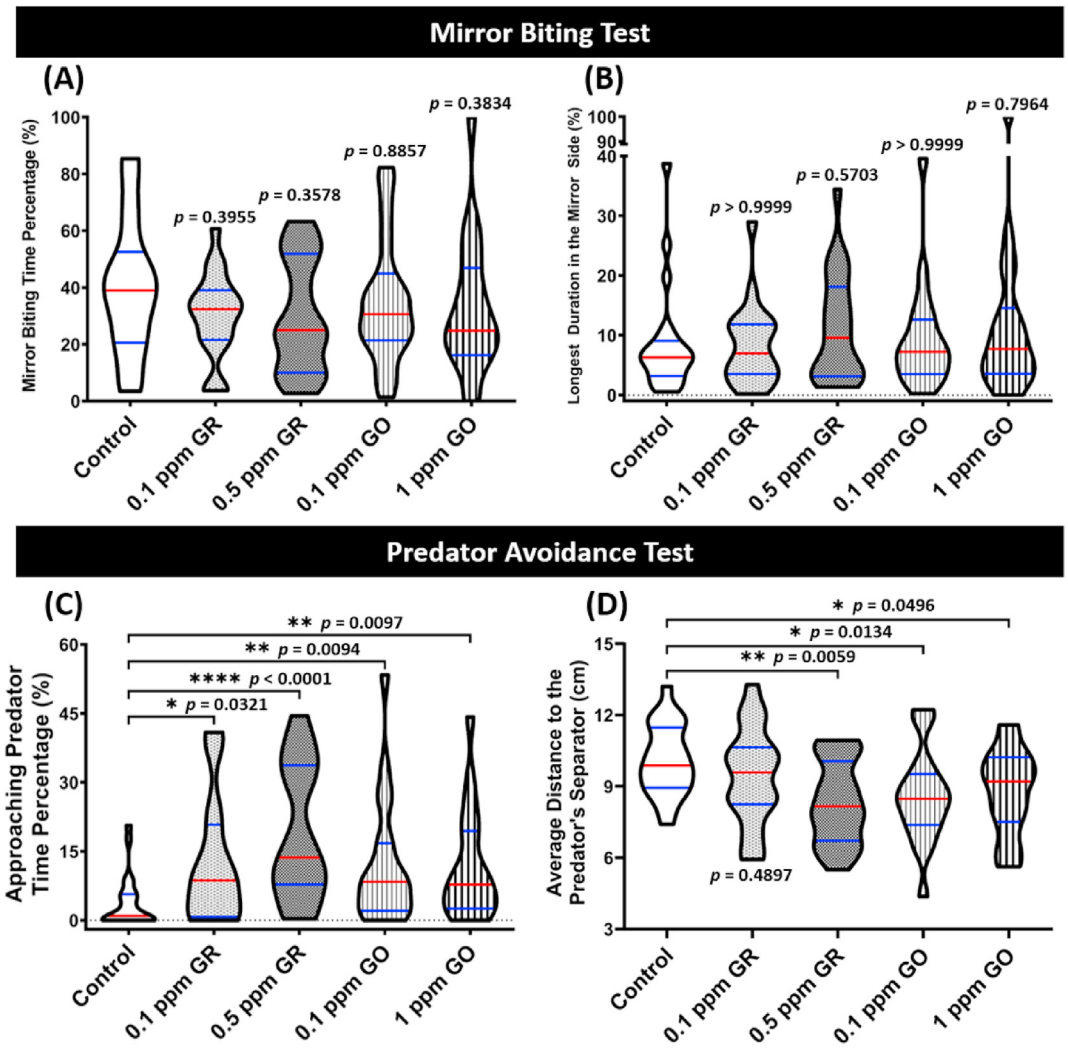

Fig. 3. Behavior endpoints comparison between control, graphene-treated, and graphene oxide-treated zebrafish groups in mirror biting and predator avoidance tests. In the mirror biting test, we analyzed (A) mirror biting time percentage and (B) longest duration in the mirror side percentage of all groups ($n = 22$ for the control and 0.5 ppm GR groups, $n = 20$ for 0.1 ppm GR and both GO groups). Meanwhile, in the predator avoidance test, we analyzed (C) approaching predator time percentage and (D) average distance to the predator separator of all groups ($n = 22$ for the control group, $n = 20$ for 0.1 ppm GR and both GO groups, $n = 21$ for 0.5 ppm GR group). In the violin plot, the median was shown by the red-colored bold line while the interquartile was shown by the blue-colored bold line. Kruskal-Wallis test continued with Dunn's multiple comparisons was used to analyze the data, except for (D), which used ordinary one-way ANOVA with Dunnett's multiple comparisons test. Statistical significances were labeled as * $p < 0.05$, ** $p < 0.01$, **** $p < 0.0001$. (For interpretation of the references to color in this figure legend, the reader is referred to the Web version of this article.)

Table 1
Comparison of neurotransmitters, antioxidant activity, and oxidative stress contents in zebrafish brain tissues quantified using enzyme-linked immunosorbent assay (ELISA) after exposure of graphene or graphene oxide. Brown-Forsythe and Welch ANOVA test with Dunnett's T3 multiple comparisons tests were used to analyze the data. The data are displayed as the mean with SD. Statistical significances were labeled as * $p < 0.05$ and ** $p < 0.01$ ($n = 5$ for all groups).

Biomarkers	Control	Graphene				Graphene Oxide				Unit
		0.1 ppm		0.5 ppm		0.1 ppm		1 ppm		
	Concentration	Concentration	*p* value	Concentration	*p* value	Concentration	*p* value	Concentration	*p* value	
5-HT	27.03 ± 7.697	34.39 ± 5.905	0.1305	15.23 ± 2.767 **	0.0232	24.77 ± 5.412	0.6085	28.64 ± 5.352	0.7110	ng/total protein (mg)
ACh	3.147 ± 0.874	3.622 ± 0.831	0.4040	1.956 ± 0.458 *	0.0354	3.334 ± 1.316	0.7996	3.380 ± 0.605	0.6396	ng/total protein (mg)
KISS	6.920 ± 2.315	8.594 ± 1.437	0.2138	5.001 ± 0.805	0.1409	7.189 ± 3.166	0.8824	7.330 ± 1.890	0.7669	ng/total protein (mg)
AChE	19.13 ± 7.015	22.57 ± 4.635	0.3910	20.85 ± 5.443	0.6772	19.54 ± 7.405	0.9307	20.76 ± 3.098	0.6534	U/total protein (mg)
DA	13.58 ± 4.321	12.33 ± 1.369	0.5668	6.816 ± 1.036 *	0.0229	12.69 ± 4.379	0.7558	15.07 ± 4.101	0.5913	pg/total protein (mg)
OT	14.19 ± 4.802	20.43 ± 3.686	0.0520	13.60 ± 1.827	0.8100	19.96 ± 11.58	0.3476	18.01 ± 3.747	0.1997	pg/total protein (mg)
Cortisol	217.7 ± 52.48	217.9 ± 36.46	0.9955	90.49 ± 14.81 **	0.0043	186 ± 36.35	0.3030	225.5 ± 41.78	0.8016	pg/total protein (mg)
ROS	75.17 ± 16.97	101.6 ± 18.34 *	0.0456	68.30 ± 14.63	0.5127	84.12 ± 29.21	0.5738	104.3 ± 12.05 *	0.0160	IU/total protein (mg)

70NPs, C-MNPs, and Fe_3O_4 MNPs behavior toxicity data from previous publications (Malhotra et al., 2019, 2020a; Sarasamma et al., 2018, 2019) were included to perform the heatmap, hierarchical clustering, and PCA comparison. PCA is one of the mathematic

methods that linearly reduce the complexity and dimension of data. Meanwhile, hierarchical clustering is an algorithm that compares both rows and so that similar rows, and similar columns, were clustered by the dendrogram, which represents their similarity. In the heatmap, a significant decrease and increase of endpoint behavior value were represented by red and blue color, respectively. Here, both PCA (Fig. 4A) and hierarchical clustering results (Fig. 4B) for GR, GO, and other nanoparticles can be separated into five major clusters (Fig. 4A&B). Mostly, each group contains a single chemical in both low and high concentrations, except in one group, consisting of C-60 NPs and C-70NPs in both concentrations. These results are indicating that each chemical has its unique pattern in altering adult zebrafish behaviors. For example, high levels of shoaling behavior-related endpoints were observed in C-60 NPs and C-70 NPs groups, while this case was not observed in the rest of the treated groups. Furthermore, a significantly decreased value of novel tank-related endpoints, especially in exploratory behavior, distinguished the Fe_3O_4 MNPs-treated groups from other treated groups. However, in both GR and GO groups, specific patterns found regarding their abnormal thigmotaxis and altered predator avoidance behavior separated them from other groups. Interestingly, both GR and GO groups were closely clustered with C-MNPs-treated groups. After further inspection, we found that even though slight alterations in zebrafish behaviors were still detected, a surface-modification in MNPs improved its biosafety and biocompatibility. This grouping is plausible since GR and GO treatment did not trigger significant alterations in zebrafish behaviors in the current study, which is somewhat similar to C-MNPs results. Overall, this result indicates that although every chemical can affect zebrafish behavior in unique fingerprint-like alteration patterns, the low and high doses of GR and GO resulted in different levels of changes than the other treatment groups, which are C-60 NPs, C-70NPs, and Fe_3O_4 MNPs, and showed more similarity to the C-MNPs group.

4. Discussion

The researches on GR and GR-related nanomaterials are essential and vital since these materials were intensively used in our daily lives, and the release of those nanomaterials to the biosphere is inevitable (Manjunatha et al., 2018). Thus, in the present study, the potential adverse effects of chronic exposure to either GR or GO were validated by using adult zebrafish at the whole organism level. From the behavioral test results, even though the treated fish exhibited similar behaviors with the untreated fish in most behavior tests, significant alterations were revealed in some zebrafish neurological behaviors. These alterations were observed mostly in their locomotor activity, exploratory behavior, and predator avoidance behavior. In elucidating the possible mechanism that underlies these phenomena, biochemical assays were conducted, and later, abnormal levels of oxidative stress, antioxidant activity, and several neurotransmitters were revealed. To the best of our knowledge, this is the first study to reveal GR and GO's adverse effects in comprehensive adult zebrafish behaviors.

In this study, significantly low levels of several neurotransmitters that are essential regulators of brain functions, including serotonin, acetylcholine, and dopamine, were observed in 0.5 ppm GR-treated group. Alterations of these neurotransmitters and their metabolites have been used to indicate toxicity in the central nervous system (CNS) (Da Rocha et al., 2019). As one of the primary neurotransmitters in the CNS, serotonin (5-hydroxytryptamine) plays an essential role in regulating a range of physiological, neuroendocrine, and behavioral processes that innervate almost all regions of the brain (Donaldson and Young, 2008; Sallinen et al., 2009). In the prior study, chronic social isolation in adult zebrafish caused a reduction in the serotonin levels in the brain of adult zebrafish and it was related to the reduction on their thigmotaxis level measured during the open-tank exploration test, which is comparable to the current results (Shams et al., 2015). Moreover, a decreased number of serotonin-containing neurons was also found in adult zebrafish's brain tissues treated with reserpine and nanosilica. Similar to our results, both treated fish also displayed inhibited exploratory behavior during the novel tank test (Li et al., 2017). A decrement in the several monoamine neurotransmitter contents in rat brain, including norepinephrine, dopamine, and serotonin also has been reported to result in depression and anxiety

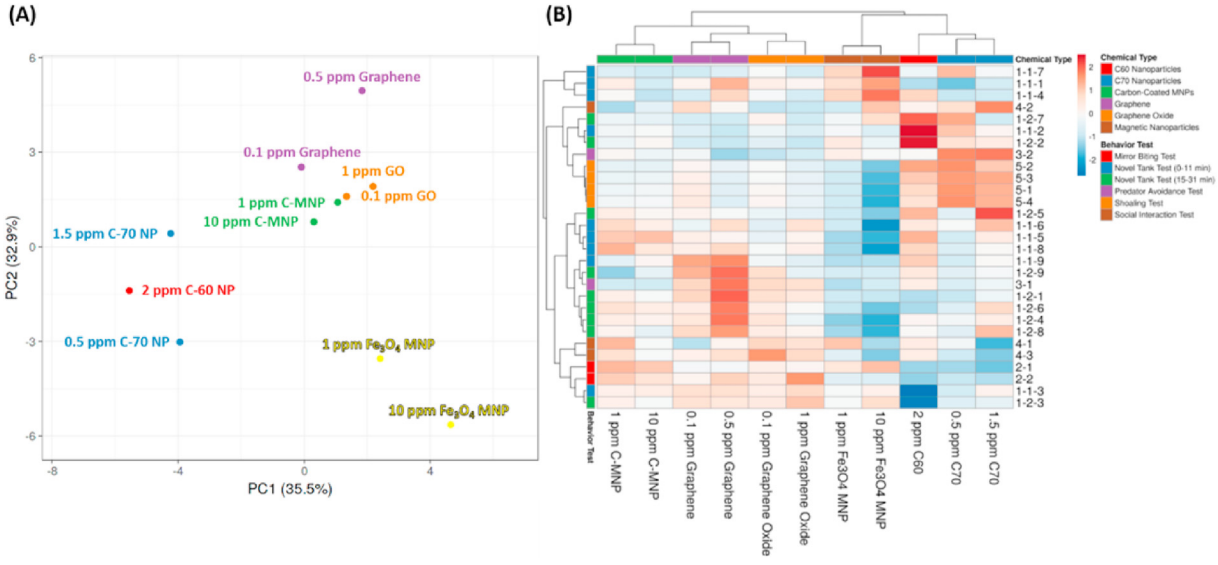

Fig. 4. (A) Principal component analysis (PCA), (B) heatmap, and hierarchical clustering analysis of multiple zebrafish behavior endpoints after exposure to graphene (purple) or graphene oxide (orange). The C-60 nanoparticle (C-60 NP, red), C-70 nanoparticle (C-70 NP, blue), Fe_3O_4 magnetic nanoparticle (Fe_3O_4 MNP, yellow), and C-MNP (carbon-coated MNP)-treated (green) groups from prior studies are included to display the different effects of both graphene and graphene oxide to these groups in terms of zebrafish behavior. In (B), the detailed behavior test code was provided in Table S2. (For interpretation of the references to color in this figure legend, the reader is referred to the Web version of this article.)

(Dixit et al., 1981; Husain et al., 1987; Ruhé et al., 2007). Furthermore, by ELISA, we found 0.5 ppm GR-treated zebrafish display reduction on the brain dopamine level. Abnormalities in dopamine, a neurotransmitter known to mediate various brain functions, have been studied in zebrafish models of impulsivity, addiction, Parkinson's disease, and schizophrenia. Decreased dopamine levels in adult zebrafish brains could be significant for long-term behavioral defects (Eddins et al., 2010). Together with serotonin results, these robust results become evidence that a high concentration of GR may affect the monoamine pathways in zebrafish since serotonin and dopamine are catalyzed by the monoamine oxidase (MAO) enzyme family (Coupland, 2001; Shams et al., 2017). The behavioral alteration observed in this group might also be related to an abnormal level of acetylcholine, a neurotransmitter of the cholinergic system that plays an important role in the CNS and the peripheral nervous system. It is related to the neuronal response's modulation by sensory stimuli and behavior (Altenhofen et al., 2017). Several prior studies found that lower levels of acetylcholine might interfere with neural signaling and lead to abnormal muscular contraction and swimming behavior (Chen et al., 2017; Guo et al., 2019; Liu et al., 2017). However, since acetylcholine is well-known for its crucial role in maintaining memory formation and participating in neural circuits related to sleep control, it is intriguing to observe the effect of a high concentration of GR in zebrafish's memory and circadian rhythm in the future (Paudel et al., 2020; Shaked et al., 2008).

Interestingly, cortisol was also found to be significantly decreased in this 0.5 ppm GR-treated group. Cortisol is used as zebrafish primary stress hormone (Cachat et al., 2010). Normally, elevated whole-body cortisol concentrations have been observed following exposure to some stressors, such as chronic crowding stress and social stress, acute net handling stress, and visual contact with a predator (Pavlidis et al., 2013). In other words, zebrafish generally show reduced anxiety-like behaviors together with a decrement in cortisol responses (Genario et al., 2020). Thus, the reduced cortisol level observed in this group might compensate for the decreased levels of other neurotransmitters found and reducing severities of behavior alterations displayed by this group. The reduced cortisol levels were also observed in the zebrafish after treated with fluoxetine, a selective serotonin reuptake inhibitor (SSRI) with robust anxiolytic effects (Egan et al., 2009). Another prior study in ketamine-treated zebrafish also discovered a similar phenomenon. In their study, ketamine, a sedative drug used in clinical and veterinary medicine to induce analgesia and anesthesia, was anxiolytic in several behavioral paradigms in adult zebrafish and tended to reduce whole-body cortisol in zebrafish (Riehl et al., 2011).

Next, regarding the GO treatment results, a significantly high ROS level was exhibited by the high concentration group. ROS is an important factor to mediate metal-induced cellular responses. When accumulated over the threshold, it can lead to malignant tumors or neoplasia (Malhotra et al., 2019). Generally, ROS levels are maintained by the action of catalase (CAT), superoxide dismutase (SOD), or glutathione peroxidase, and some adverse effects, including membrane peroxidation and DNA strand breakage may occur if ROS levels cannot be reduced by those cellular antioxidant activities (Di Giulio et al., 1989). In line with our results, a prior study in zebrafish revealed that while GR showed a stronger ability to decrease the survival rate and induce acute toxicity, GO showed apparent toxicity in terms of ROS generation. The toxicity of GO is more superior to GR to activate BER and PI3K pathways that are known as response pathways for DNA damages, external injuries, and inflammation (Jia et al., 2019b). In another study, cytotoxicity was also demonstrated by GO through ROS generation. This phenomenon resulted in impaired mitochondrial respiration and cell apoptosis (Duch et al., 2011). In addition, GO was toxic to MCF-7 cells in a dose-dependent manner by increasing ROS generation and decreasing cell viability (Chen et al., 2016). Furthermore, the generation of ROS and swimming impairment observed during this study was in line with a previous study in water flea *Daphnia magna.* After 72 h of GO treatments, an overall decrease was seen in their swimming velocity simultaneously with ROS generation (Cano et al., 2017). This phenomenon is plausible since, in the zebrafish larvae, the increase of ROS could render zebrafish brain development and subsequently affect the swimming behavior. In contrast, in adult zebrafish, ROS production in the brain might damage the brain and neurons and could lead to severe swimming defects (Kim et al., 2011; Salminen and Paul, 2014). This finding might also elucidate the swimming impairment exhibited by the low concentration of GR and GO-treated groups, even though it was not as severe as the 1 ppm GO group. The ROS level was slightly elevated in these low concentration groups, even though it did not reach statistical differences. Additionally, altered swimming activity might also occur since oxidative stress caused by GO interactions will cell membranes was found to increase the number of zebrafish gills cells that undergo apoptosis and necrosis (Souza et al., 2017). However, even though an elevated level of ROS was clearly shown here, the oxidative toxicity of these particles is needed to be further confirmed by measuring a vital first-line defense system against oxidative toxicity, which are SOD and CAT, and some indicators for lipid peroxidation of zebrafish, such as MDA.

Notably, the most interesting result in the current study was the alteration in zebrafish predator avoidance behavior observed in all treated groups. An alteration in antipredator response can affect fish survivability in nature. This result might indicate that chronic exposure of both GR and GO can diminish zebrafish fear response. Fear is defined as a set of responses directly induced by the appearance of specific aversive stimuli, and regulation of fear-related behaviors in animal models is well known to be involved by different neurotransmitter systems (Guilherme Graeff et al., 2015; Nowicki et al., 2014). One of the commonly used neurotransmitter systems to assess animals fear-related behavior is the serotonergic neurotransmission system, which plays a role in the control of the defensive reaction, including decreasing fear-like behavior in mammals that putatively mediated by the periaqueductal gray (Graeff et al., 1997; Maximino et al., 2013; Nowicki et al., 2014). Furthermore, recent studies also demonstrated that acetylcholine might also be associated with fear-related behavior via nicotinic or muscarinic receptors (Canzian et al., 2017). However, even though they possessed an impaired predator avoidance behavior, there was no significant difference between the serotonin and acetylcholine levels between control and treated groups, except in the high concentration GR-treated group. These results may be due to numerous factors modulate the regulation of fear reaction. Many studies have demonstrated the regulatory role of sex hormones on the synthesis and secretion of glucocorticoids, which play key roles in regulating several reactions, including fear reaction (Tu et al., 2020). Kisspeptin has proven for its significant part in vertebrate reproduction. Furthermore, this hypothalamic neuropeptide has been demonstrated for its unique role in altering fear response in several animal models, including mice and zebrafish. Several hormones, such as vasopressin and oxytocin, which are notable as modulators of various emotional and cognitive processes, including fear, might also be related to this behavioral impairment (Campbell et al., 2009). Moreover, a pioneer study found that behavioral components of fear by oxytocin were associated with amygdala coupling to brainstem centers and reduced activation of it (De Dreu et al., 2012). Further, the dampened predator avoidance behavior in the treated fish might also related

Table 2
The summary of several GR- and GO-treated zebrafish behavioral and biochemical differences compared with the untreated group. The signatures of the zebrafish behavioral and biochemical tests are summarized (↑: upregulated, ↓: downregulated, -: no difference, numbers of the arrow in zebrafish behavior endpoints represent the number of altered behavior endpoints from each behavioral test while numbers of the arrow in biomarkers represent the significances of altered biomarker levels from each ELISA).

		Graphene		Graphene Oxide	
		0.1 ppm	0.5 ppm	0.1 ppm	1 ppm
Zebrafish Behavior Endpoints	Locomotor Activity	↓↓↓	-	↓↓	↓↓↓
	Exploratory Behavior	↓	↓	-	-
	Aggressiveness	-	-	-	-
	Predator Avoidance	↓	↓↓	↓↓	↓↓
	Conspecific Social Interaction	-	-	-	-
	Shoaling Size	-	-	-	-
Biomarkers	5-HT	-	↓	-	-
	ACh	-	↓	-	-
	Kisspeptin	-	-	-	-
	AChE	-	-	-	-
	Dopamine	-	↓	-	-
	Oxytocin	-	-	-	-
	Cortisol	-	↓↓	-	-
	ROS	↑	-	-	↑

to γ-aminobutyric acid (GABA) since a prior study in the nucleus accumbens shell rats discovered that GABA neurotransmission was responsible for fear-related or defensive behavior (Reynolds and Berridge, 2001). Thus, future studies are needed to examine several neurotransmitters that might contribute to the predator avoidance behavior impairment after GR and GO treatments.

Up to now, the behavior toxicity approach to assess the toxicities of GR and GO in adult zebrafish has not yet been studied extensively. Here, a phenomic analysis was performed to evaluate the risk of GR or GO exposure based on each zebrafish behavioral endpoint in every behavior assays. Based on the hierarchical clustering, GR in both concentrations were grouped in a different cluster with GO groups, which indicated that each GR and GO has its unique pattern in altering zebrafish behaviors. These differences are plausible since GR and GO have different chemical and physical properties. GR is more hydrophobic and prone to aggregate in an aqueous environment while GO, on the other hand, has hydrophilic nature. In addition, the functional groups present on the GO surface have been found to generate different toxic effects from the non-functionalized GR in pure culture studies. Moreover, these functional groups make the nanomaterial more prone to interact with heavy metal, biomacromolecules, and other contaminants in the water (Carpio et al., 2014; Nguyen et al., 2017; Smith et al., 2014; Zhao et al., 2011). A prior study demonstrated that GR and GO affected the microbial communities in the activated sludge differently regarding these differences. They found that GO exhibited higher toxic effects to the sludge microbial community than GR because GO presented the highest impact in nutrient removal, gene abundance, and changes in microbial population structure (Nguyen and Rodrigues, 2018). The differences between these two graphene materials based on their effects on copper (Cu) toxicity in *Daphnia magna* were also studied before. In their study, while GR remarkably increased Cu accumulation and enhanced the oxidative stress injury, GO significantly decreased the Cu accumulation and alleviated the oxidative stress injury caused by Cu. Later, it was found that the fundamental factor for the differences was the surface oxygenic functional groups, which is a primary variable that determines the adsorption capacity of graphene materials (Liu et al., 2018). Furthermore, both GR and GO groups displayed a diverse pattern that distinguishes them from other nanoparticles that were studied previously, including C-60, C-70, Fe_3O_4, and carbon-coated magnetic NPs. The notable possibility is that GR-based materials are unique and possess significantly different properties than spherical nanoparticles and one-dimensional carbon nanotubes (Seabra et al., 2014). Interestingly, they were closely clustered with C-MNP groups, which possessed better biosafety than the uncoated MNPs (Malhotra et al., 2020a). This grouping might indicate the less severity of GR and GO in terms of zebrafish behavior alterations compared to other nanoparticles, which are C-60 NPs, C-70 NPs, and Fe_3O_4 MNPs (Malhotra et al., 2019; Sarasamma et al., 2018, 2019). However, ones have to note that the differences may be due to the different concentrations of some nanoparticles used in the prior studies. Thus, further studies are required to compare the behavioral toxicities of GR, GO, and other commonly used materials better. Nevertheless, the GR and GO's toxicities are still cannot be neglected and should be carefully addressed in the future.

5. Conclusions

Considering the increasing applications of GR and GO in industry and biomedicine, the toxicities of these materials should be evaluated. In summary, this is the first study showing evidence of waterborne GR and GO exposure in causing abnormal behaviors in adult zebrafish and induced oxidative stress, antioxidant activity, and neurotransmitter changes in the zebrafish brain (summarized in Table 2). After administering the GR and GO to adult zebrafish consecutively for ~14 days, we found that exposure of GR or GO caused behavior alterations, such as diminished predator avoidance behavior, abnormal exploratory behavior, and lower locomotor activities. The behavior alterations observed might be caused by the abnormal levels of several neurotransmitters and antioxidant activity exhibited by the treated fish. Nevertheless, since numerous factors modulate zebrafish behaviors, future studies are needed to examine several neurotransmitters that might contribute to the zebrafish behavior impairments caused by these materials. Furthermore, due to the different chemical and physical properties of GR and GO, they displayed unique patterns in terms of altering zebrafish behaviors that distinguished them from each other. Interestingly, a less toxic effect of both GR and GO than other nanomaterials tested in previous studies was observed at behavioral levels in zebrafish. However, the potential tissue-specific toxicities of both GR and GO cannot be neglected. Thus, more studies on different parameters of environmental condition, dosage, and exposure duration are needed to further evaluate the safety and toxicity of using these nanomaterials.

Funding

This study was funded by the grants sponsored by the Ministry of Science and Technology MOST 108-2313-B-033-001-MY3 and

MOST 107-2622-B-033-001-CC2 to C.-D.H.

Author contributions

J.-S.L. and C.-D.H. participated in the study design. G.A. and P.S. performed data curation and formal analysis. C.-D.H. provided funding acquisition and project administration. N.M., M.J.M.R., and Y.H. performed the investigation, methodology, and provided resources. J.-C.H., K.H.-C.C. H.-S.H., and T.-R.G. performed visualization. J.-S.L. and C.-D.H. wrote the original draft.

Novelty statement

In this paper, we performed a multiple dimensional behavioral phenomic analysis of the toxicities of graphene and graphene oxide at environmentally relevant concentration. By using the phenomic approach, we were able to systematically compare the toxicity of graphene and graphene oxide to adult zebrafish at a neurobehavioral level for the first time. Our results provided new evidence for the adverse consequences of graphene and graphene oxide induced zebrafish behavioral dysregulation and these assessments can contribute to our understanding of graphene and graphene oxide biosafety.

Declaration of competing interest

The authors declare that they have no known competing financial interests or personal relationships that could have appeared to influence the work reported in this paper.

Acknowledgments

We thank Taiwan Zebrafish Core Facility at Academia Sinica (TZCAS) to provide zebrafish AB strain. All authors reviewed the manuscript. We also appreciate the anonymous reviewers and editors for their professional comments, which improved the quality of this paper.

Appendix A. Supplementary data

Supplementary data to this article can be found online at https://doi.org/10.1016/j.envpol.2021.116907.

References

Adams, D.C., Anthony, C.D., 1996. Using randomization techniques to analyse behavioural data. Anim. Behav. 51, 733–738.
Ahmed, O., Seguin, D., Gerlai, R., 2011. An automated predator avoidance task in zebrafish. Behav. Brain Res. 216, 166–171.
Ain, Q.T., Haq, S.H., Alshammari, A., Al-Mutlaq, M.A., Anjum, M.N., 2019. The systemic effect of PEG-nGO-induced oxidative stress in vivo in a rodent model. Beilstein J. Nanotechnol. 10, 901–911.
Aleström, P., D'Angelo, L., Midtlyng, P.J., Schorderet, D.F., Schulte-Merker, S., Sohm, F., Warner, S., 2019. Zebrafish: housing and husbandry recommendations. Lab. Anim, 0023677219869037.
Altenhofen, S., Nabinger, D.D., Wiprich, M.T., Pereira, T.C.B., Bogo, M.R., Bonan, C.D., 2017. Tebuconazole alters morphological, behavioral and neurochemical parameters in larvae and adult zebrafish (Danio rerio). Chemosphere 180, 483–490.
Audira, G., Ngoc Anh, N.T., Ngoc Hieu, B.T., Malhotra, N., Siregar, P., Villalobos, O., Villaflores, O.B., Ger, T.-R., Huang, J.-C., Chen, K.H.-C., 2020a. Evaluation of the adverse effects of chronic exposure to donepezil (an acetylcholinesterase inhibitor) in adult zebrafish by behavioral and biochemical assessments. Biomolecules 10, 1340.
Audira, G., Sampurna, B., Juniardi, S., Liang, S.-T., Lai, Y.-H., Hsiao, C.-D., 2018. A versatile setup for measuring multiple behavior endpoints in zebrafish. Inventions 3, 75.
Audira, G., Siregar, P., Chen, J.-R., Lai, Y.-H., Huang, J.-C., Hsiao, C.-D., 2020b. Systematical exploration of the common solvent toxicity at whole organism level by behavioral phenomics in adult zebrafish. Environ. Pollut. 115239.
Avdesh, A., Chen, M., Martin-Iverson, M.T., Mondal, A., Ong, D., Rainey-Smith, S., Taddei, K., Lardelli, M., Groth, D.M., Verdile, G., 2012. Regular care and maintenance of a zebrafish (Danio rerio) laboratory: an introduction. JoVE, e4196.
Buenafe, O.E., Orellana-Paucar, A., Maes, J., Huang, H., Ying, X., De Borggraeve, W., Crawford, A.D., Luyten, W., Esguerra, C.V., de Witte, P., 2013. Tanshinone IIA exhibits anticonvulsant activity in zebrafish and mouse seizure models. ACS Chem. Neurosci. 4, 1479–1487.
Cachat, J., Stewart, A., Grossman, L., Gaikwad, S., Kadri, F., Chung, K.M., Wu, N., Wong, K., Roy, S., Suciu, C., 2010. Measuring behavioral and endocrine responses to novelty stress in adult zebrafish. Nat. Protoc. 5, 1786.
Campbell, P., Ophir, A.G., Phelps, S.M., 2009. Central vasopressin and oxytocin receptor distributions in two species of singing mice. J. Comp. Neurol. 516, 321–333.
Cano, A.M., Maul, J.D., Saed, M., Shah, S.A., Green, M.J., Cañas-Carrell, J.E., 2017. Bioaccumulation, stress, and swimming impairment in Daphnia magna exposed to multiwalled carbon nanotubes, graphene, and graphene oxide. Environ. Toxicol. Chem. 36, 2199–2204.
Canzian, J., Fontana, B.D., Quadros, V.A., Rosemberg, D.B., 2017. Conspecific alarm substance differently alters group behavior of zebrafish populations: putative involvement of cholinergic and purinergic signaling in anxiety-and fear-like responses. Behav. Brain Res. 320, 255–263.
Carpio, I.E.M., Mangadlao, J.D., Nguyen, H.N., Advincula, R.C., Rodrigues, D.F., 2014. Graphene oxide functionalized with ethylenediamine triacetic acid for heavy metal adsorption and anti-microbial applications. Carbon 77, 289–301.
Chen, B., Liu, M., Zhang, L., Huang, J., Yao, J., Zhang, Z., 2011. Polyethylenimine-functionalized graphene oxide as an efficient gene delivery vector. J. Mater. Chem. 21, 7736–7741.
Chen, L., Wang, X., Zhang, X., Lam, P.K., Guo, Y., Lam, J.C., Zhou, B., 2017. Transgenerational endocrine disruption and neurotoxicity in zebrafish larvae after parental exposure to binary mixtures of decabromodiphenyl ether (BDE-209) and lead. Environ. Pollut. 230, 96–106.
Chen, M., Yin, J., Liang, Y., Yuan, S., Wang, F., Song, M., Wang, H., 2016. Oxidative stress and immunotoxicity induced by graphene oxide in zebrafish. Aquat. Toxicol. 174, 54–60.
Coupland, N.J., 2001. Social phobia: etiology, neurobiology, and treatment. J. Clin. Psychiatr.
Da Rocha, A., Kist, L., Almeida, E., Silva, D., Bonan, C., Altenhofen, S., Kaufmann Jr., C., Bogo, M., Barros, D., Oliveira, S., 2019. Neurotoxicity in zebrafish exposed to carbon nanotubes: effects on neurotransmitters levels and antioxidant system. Comp. Biochem. Physiol. C Toxicol. Pharmacol. 218, 30–35.
de Abreu, M.S., Giacomini, A.C., dos Santos, B.E., Genario, R., Marchiori, N.I., da Rosa, L.G., Kalueff, A.V., 2019. Effects of lidocaine on adult zebrafish behavior and brain acetylcholinesterase following peripheral and systemic administration. Neurosci. Lett. 692, 181–186.
De Dreu, C.K., Shalvi, S., Greer, L.L., Van Kleef, G.A., Handgraaf, M.J., 2012. Oxytocin motivates non-cooperation in intergroup conflict to protect vulnerable in-group members. PloS One 7, e46751.
Di Giulio, R.T., Washburn, P.C., Wenning, R.J., Winston, G.W., Jewell, C.S., 1989. Biochemical responses in aquatic animals: a review of determinants of oxidative stress. Environ. Toxicol. Chem.: Int. J. 8, 1103–1123.
Ding, J., Li, B., Liu, Y., Yan, X., Zeng, S., Zhang, X., Hou, L., Cai, Q., Zhang, J., 2015. Fabrication of Fe_3O_4@ reduced graphene oxide composite via novel colloid electrostatic self-assembly process for removal of contaminants from water. J. Mater. Chem. 3, 832–839.
Dixit, R., Husain, R., Mukhtar, H., Seth, P.K., 1981. Effect of acrylamide on biogenic amine levels, monoamine oxidase, and cathepsin D activity of rat brain. Environ. Res. 26, 168–173.
Donaldson, Z.R., Young, L.J., 2008. Oxytocin, vasopressin, and the neurogenetics of sociality. Science 322, 900–904.
Duch, M.C., Budinger, G.S., Liang, Y.T., Soberanes, S., Urich, D., Chiarella, S.E., Campochiaro, L.A., Gonzalez, A., Chandel, N.S., Hersam, M.C., 2011. Minimizing oxidation and stable nanoscale dispersion improves the biocompatibility of graphene in the lung. Nano Lett. 11, 5201–5207.
Eddins, D., Cerutti, D., Williams, P., Linney, E., Levin, E.D., 2010. Zebrafish provide a sensitive model of persisting neurobehavioral effects of developmental chlorpyrifos exposure: comparison with nicotine and pilocarpine effects and relationship to dopamine deficits. Neurotoxicol. Teratol. 32, 99–108.
Egan, R.J., Bergner, C.L., Hart, P.C., Cachat, J.M., Canavello, P.R., Elegante, M.F., Elkhayat, S.I., Bartels, B.K., Tien, A.K., Tien, D.H., 2009. Understanding behavioral and physiological phenotypes of stress and anxiety in zebrafish. Behav. Brain Res. 205, 38–44.
Fernandes, A.L., Nascimento, J.P., Santos, A.P., Furtado, C.A., Romano, L.A., da Rosa, C.E., Monserrat, J.M., Ventura-Lima, J., 2018. Assessment of the effects of graphene exposure in Danio rerio: a molecular, biochemical and histological approach to investigating mechanisms of toxicity. Chemosphere 210, 458–466.
Furue, R., Koveke, E.P., Sugimoto, S., Shudo, Y., Hayami, S., Ohira, S.-I., Toda, K., 2017. Arsine gas sensor based on gold-modified reduced graphene oxide. Sensor. Actuator. B Chem. 240, 657–663.
Gao, Y., Shiue, R.-J., Gan, X., Li, L., Peng, C., Meric, I., Wang, L., Szep, A., Walker Jr., D., Hone, J., 2015. High-speed electro-optic modulator integrated with graphene-boron nitride heterostructure and photonic crystal nanocavity. Nano Lett. 15, 2001–2005.
Geim, A.K., 2009. Graphene: status and prospects. Science 324, 1530–1534.
Genario, R., Giacomini, A.C., de Abreu, M.S., Marcon, L., Demin, K.A., Kalueff, A.V., 2020. Sex differences in adult zebrafish anxiolytic-like responses to diazepam and melatonin. Neurosci. Lett. 714, 134548.

Goodwin Jr., D.G., Adeleye, A.S., Sung, L., Ho, K.T., Burgess, R.M., Petersen, E.J., 2018. Detection and quantification of graphene-family nanomaterials in the environment. Environ. Sci. Technol. 52, 4491–4513.
Graeff, F.G., Viana, M.B., Mora, P.O., 1997. Dual role of 5-HT in defense and anxiety. Neurosci. Biobehav. Rev. 21, 791–799.
Guilherme Graeff, F., Beatriz Sant'Ana, A., Helena Vilela-Costa, H., Zangrossi Jr., H., 2015. New findings on the neurotransmitter modulation of defense in the dorsal periaqueductal gray. CNS Neurol. Disord. - Drug Targets 14, 988–995.
Guo, Y., Chen, L., Wu, J., Hua, J., Yang, L., Wang, Q., Zhang, W., Lee, J.-S., Zhou, B., 2019. Parental co-exposure to bisphenol A and nano-TiO2 causes thyroid endocrine disruption and developmental neurotoxicity in zebrafish offspring. Sci. Total Environ. 650, 557–565.
Hu, M., Yao, Z., Hui, K., Hui, K., 2017a. Novel mechanistic view of catalytic ozonation of gaseous toluene by dual-site kinetic modelling. Chem. Eng. J. 308, 710–718.
Hu, M., Yao, Z., Wang, X., 2017b. Characterization techniques for graphene-based materials in catalysis. AIMS Mater. Sci. 4, 755.
Huh, S.H., 2014. X-ray diffraction of multi-layer graphenes: instant measurement and determination of the number of layers. Carbon 78, 617–621.
Husain, R., Dixit, R., Das, M., Seth, P.K., 1987. Neurotoxicity of acrylamide in developing rat brain: changes in the levels of brain biogenic amines and activities of monoamine oxidase and acetylcholine esterase. Ind. Health 25, 19–28.
Jia, P.-P., Sun, T., Junaid, M., Xiong, Y.-H., Wang, Y.-Q., Liu, L., Pu, S.-Y., Pei, D.-S., 2019a. Chronic exposure to graphene oxide (GO) induced inflammation and differentially disturbed the intestinal microbiota in zebrafish. Environ. Sci.: Nano 6, 2452–2469.
Jia, P.-P., Sun, T., Junaid, M., Yang, L., Ma, Y.-B., Cui, Z.-S., Wei, D.-P., Shi, H.-F., Pei, D.-S., 2019b. Nanotoxicity of different sizes of graphene (G) and graphene oxide (GO) in vitro and in vivo. Environ. Pollut. 247, 595–606.
Johra, F.T., Lee, J.-W., Jung, W.-G., 2014. Facile and safe graphene preparation on solution based platform. J. Ind. Eng. Chem. 20, 2883–2887.
Kalueff, A.V., Echevarria, D.J., Homechaudhuri, S., Stewart, A.M., Collier, A.D., Kaluyeva, A.A., Li, S., Liu, Y., Chen, P., Wang, J., 2016. Zebrafish neurobehavioral phenomics for aquatic neuropharmacology and toxicology research. Aquat. Toxicol. 170, 297–309.
Khurana, G., Misra, P., Kumar, N., Katiyar, R.S., 2014. Tunable power switching in nonvolatile flexible memory devices based on graphene oxide embedded with ZnO nanorods. J. Phys. Chem. C 118, 21357–21364.
Kim, J.-Y., Seo, J., Cho, K.-H., 2011. Aspartame-fed zebrafish exhibit acute deaths with swimming defects and saccharin-fed zebrafish have elevation of cholesteryl ester transfer protein activity in hypercholesterolemia. Food Chem. Toxicol. 49, 2899–2905.
Kim, K.L., Lee, W., Hwang, S.K., Joo, S.H., Cho, S.M., Song, G., Cho, S.H., Jeong, B., Hwang, I., Ahn, J.-H., 2016. Epitaxial growth of thin ferroelectric polymer films on graphene layer for fully transparent and flexible nonvolatile memory. Nano Lett. 16, 334–340.
Kolesnikova, T.O., Khatsko, S.L., Eltsov, O.S., Shevyrin, V.A., Kalueff, A.V., 2019. When fish take a bath: psychopharmacological characterization of the effects of a synthetic cathinone bath salt 'flakka'on adult zebrafish. Neurotoxicol. Teratol. 73, 15–21.
Kostiuk, D., Bodik, M., Siffalovic, P., Jergel, M., Halahovets, Y., Hodas, M., Pelletta, M., Pelach, M., Hulman, M., Spitalsky, Z., 2016. Reliable determination of the few-layer graphene oxide thickness using Raman spectroscopy. J. Raman Spectrosc. 47, 391–394.
Kuhn, M., Johnson, K., 2019. Feature Engineering and Selection: A Practical Approach for Predictive Models. CRC Press.
Lai, Q., Zhu, S., Luo, X., Zou, M., Huang, S., 2012. Ultraviolet-visible spectroscopy of graphene oxides. AIP Adv. 2, 032146.
Lawrence, C., 2007. The husbandry of zebrafish (Danio rerio): a review. Aquaculture 269, 1–20.
Layek, R.K., Nandi, A.K., 2013. A review on synthesis and properties of polymer functionalized graphene. Polymer 54, 5087–5103.
Li, X., Liu, X., Li, T., Li, X., Feng, D., Kuang, X., Xu, J., Zhao, X., Sun, M., Chen, D., 2017. SiO 2 nanoparticles cause depression and anxiety-like behavior in adult zebrafish. RSC Adv. 7, 2953–2963.
Liu, J., Zhou, Y., Qi, X., Chen, J., Chen, W., Qiu, G., Wu, Z., Wu, N., 2017. CRISPR/Cas9 in zebrafish: an efficient combination for human genetic diseases modeling. Hum. Genet. 136, 1–12.
Liu, Y., Fan, W., Xu, Z., Peng, W., Luo, S., 2018. Comparative effects of graphene and graphene oxide on copper toxicity to Daphnia magna: role of surface oxygenic functional groups. Environ. Pollut. 236, 962–970.
Malhotra, N., Audira, G., Chen, J.-R., Siregar, P., Hsu, H.-S., Lee, J.-S., Ger, T.-R., Hsiao, C.-D., 2020a. Surface modification of magnetic nanoparticles by carbon-coating can increase its biosafety: evidences from biochemical and neurobehavioral tests in zebrafish. Molecules 25, 2256.
Malhotra, N., Chen, J.-R., Sarasamma, S., Audira, G., Siregar, P., Liang, S.-T., Lai, Y.-H., Lin, G.-M., Ger, T.-R., Hsiao, C.-D., 2019. Ecotoxicity assessment of Fe3O4 magnetic nanoparticle exposure in adult zebrafish at an environmental pertinent concentration by behavioral and biochemical testing. Nanomaterials 9, 873.
Malhotra, N., Villaflores, O.B., Audira, G., Siregar, P., Lee, J.-S., Ger, T.-R., Hsiao, C.-D., 2020b. Toxicity studies on graphene-based nanomaterials in aquatic organisms: current understanding. Molecules 25, 3618.
Manjunatha, B., Park, S.H., Kim, K., Kundapur, R.R., Lee, S.J., 2018. Pristine graphene induces cardiovascular defects in zebrafish (Danio rerio) embryogenesis. Environ. Pollut. 243, 246–254.
Markovic, M., Kumar, A., Andjelkovic, I., Lath, S., Kirby, J.K., Losic, D., Batley, G.E., McLaughlin, M.J., 2018. Ecotoxicology of manufactured graphene oxide nanomaterials and derivation of preliminary guideline values for freshwater environments. Environ. Toxicol. Chem. 37, 1340–1348.
Maximino, C., Puty, B., Benzecry, R., Araújo, J., Lima, M.G., Batista, E.d.J.O., de Matos Oliveira, K.R., Crespo-Lopez, M.E., Herculano, A.M., 2013. Role of serotonin in zebrafish (Danio rerio) anxiety: relationship with serotonin levels and effect of buspirone, WAY 100635, SB 224289, fluoxetine and para-chlorophenylalanine (pCPA) in two behavioral models. Neuropharmacology 71, 83–97.
Mendoza-Sánchez, B., Gogotsi, Y., 2016. Synthesis of two-dimensional materials for capacitive energy storage. Adv. Mater. 28, 6104–6135.
Metsalu, T., Vilo, J., 2015. ClustVis: a web tool for visualizing clustering of multivariate data using Principal Component Analysis and heatmap. Nucleic Acids Res. 43, W566–W570.
Moretz, J.A., Martins, E.P., Robison, B.D., 2007. The effects of early and adult social environment on zebrafish (Danio rerio) behavior. Environ. Biol. Fish. 80, 91–101.
Munz, M., Giusca, C.E., Myers-Ward, R.L., Gaskill, D.K., Kazakova, O., 2015. Thickness-dependent hydrophobicity of epitaxial graphene. ACS Nano 9, 8401–8411.
Nguyen, H.N., Nadres, E.T., Alamani, B.G., Rodrigues, D.F., 2017. Designing polymeric adhesives for antimicrobial materials: poly (ethylene imine) polymer, graphene, graphene oxide and molybdenum trioxide—a biomimetic approach. J. Mater. Chem. B 5, 6616–6628.
Nguyen, H.N., Rodrigues, D.F., 2018. Chronic toxicity of graphene and graphene oxide in sequencing batch bioreactors: a comparative investigation. J. Hazard Mater. 343, 200–207.
Ni, H., Peng, L., Gao, X., Ji, H., Ma, J., Li, Y., Jiang, S., 2019. Effects of maduramicin on adult zebrafish (Danio rerio): acute toxicity, tissue damage and oxidative stress. Ecotoxicol. Environ. Saf. 168, 249–259.
Nouara, A., Wu, Q., Li, Y., Tang, M., Wang, H., Zhao, Y., Wang, D., 2013. Carboxylic acid functionalization prevents the translocation of multi-walled carbon nanotubes at predicted environmentally relevant concentrations into targeted organs of nematode Caenorhabditis elegans. Nanoscale 5, 6088–6096.
Novoselov, K.S., Geim, A., 2007. The rise of graphene. Nat. Mater. 6, 183–191.
Nowicki, M., Tran, S., Muraleetharan, A., Markovic, S., Gerlai, R., 2014. Serotonin antagonists induce anxiolytic and anxiogenic-like behavior in zebrafish in a receptor-subtype dependent manner. Pharmacol. Biochem. Behav. 126, 170–180.
Orellana-Paucar, A.M., Afrikanova, T., Thomas, J., Aibuldinov, Y.K., Dehaen, W., de Witte, P.A., Esguerra, C.V., 2013. Insights from zebrafish and mouse models on the activity and safety of ar-turmerone as a potential drug candidate for the treatment of epilepsy. PloS One 8, e81634.
Pan, S., Aksay, I.A., 2011. Factors controlling the size of graphene oxide sheets produced via the graphite oxide route. ACS Nano 5, 4073–4083.
Paredes, J., Villar-Rodil, S., 2016. Biomolecule-assisted exfoliation and dispersion of graphene and other two-dimensional materials: a review of recent progress and applications. Nanoscale 8, 15389–15413.
Park, S., Ruoff, R.S., 2009. Chemical methods for the production of graphenes. Nat. Nanotechnol. 4, 217–224.
Paudel, Y.N., Kumari, Y., Abidin, S.A.Z., Othman, I., Shaikh, M., 2020. Pilocarpine induced behavioral and biochemical alterations in chronic seizure-like condition in adult zebrafish. Int. J. Mol. Sci. 21, 2492.
Pavlidis, M., Digka, N., Theodoridi, A., Campo, A., Barsakis, K., Skouradakis, G., Samaras, A., Tsalafouta, A., 2013. Husbandry of zebrafish, Danio rerio, and the cortisol stress response. Zebrafish 10, 524–531.
Pavlov, D., Kasumyan, A., 2000. Patterns and mechanisms of schooling behavior in fish: a review. J. Ichthyol. 40, S163.
Pérez-Escudero, A., Vicente-Page, J., Hinz, R.C., Arganda, S., De Polavieja, G.G., 2014. idTracker: tracking individuals in a group by automatic identification of unmarked animals. Nat. Methods 11, 743.
Perrozzi, F., Prezioso, S., Ottaviano, L., 2014. Graphene oxide: from fundamentals to applications. J. Phys. Condens. Matter 27, 013002.
Privitera, G.J., 2015. Student Study Guide with IBM® SPSS® Workbook for Essential Statistics for the Behavioral Sciences. SAGE Publications.
Qiang, L., Chen, M., Zhu, L., Wu, W., Wang, Q., 2016. Facilitated bioaccumulation of perfluorooctanesulfonate in common carp (Cyprinus carpio) by graphene oxide and remission mechanism of fulvic acid. Environ. Sci. Technol. 50, 11627–11636.
Reynolds, S.M., Berridge, K.C., 2001. Fear and feeding in the nucleus accumbens shell: rostrocaudal segregation of GABA-elicited defensive behavior versus eating behavior. J. Neurosci. 21, 3261–3270.
Riehl, R., Kyzar, E., Allain, A., Green, J., Hook, M., Monnig, L., Rhymes, K., Roth, A., Pham, M., Razavi, R., 2011. Behavioral and physiological effects of acute ketamine exposure in adult zebrafish. Neurotoxicol. Teratol. 33, 658–667.
Ruhé, H.G., Mason, N.S., Schene, A.H., 2007. Mood is indirectly related to serotonin, norepinephrine and dopamine levels in humans: a meta-analysis of monoamine depletion studies. Mol. Psychiatr. 12, 331–359.
Sajibul, M., Bhuyan, A., Uddin, M.N., Islam, M.M., Bipasha, F.A., Hossain, S.S., 2016. Synthesis of graphene. Int. Nano Lett. 6, 65.
Salkind, N.J., 2009. Statistics for People Who (Think They) Hate Statistics: Excel 2007 Edition. SAGE.
Sallinen, V., Sundvik, M., Reenilä, I., Peitsaro, N., Khrustalyov, D., Anichtchik, O., Toleikyte, G., Kaslin, J., Panula, P., 2009. Hyperserotonergic phenotype after monoamine oxidase inhibition in larval zebrafish. J. Neurochem. 109, 403–415.
Salminen, L.E., Paul, R.H., 2014. Oxidative stress and genetic markers of suboptimal antioxidant defense in the aging brain: a theoretical review. Rev. Neurosci. 25, 805–819.
Sarasamma, S., Audira, G., Juniardi, S., Sampurna, B., Lai, Y.-H., Hao, E., Chen, J.-R.,

Hsiao, C.-D., 2018. Evaluation of the effects of carbon 60 nanoparticle exposure to adult zebrafish: a behavioral and biochemical approach to elucidate the mechanism of toxicity. Int. J. Mol. Sci. 19, 3853.
Sarasamma, S., Audira, G., Samikannu, P., Juniardi, S., Siregar, P., Hao, E., Chen, J.-R., Hsiao, C.-D., 2019. Behavioral impairments and oxidative stress in the brain, muscle, and gill caused by chronic exposure of C70 nanoparticles on adult zebrafish. Int. J. Mol. Sci. 20, 5795.
Sawle, A.D., Wit, E., Whale, G., Cossins, A.R., 2010. An information-rich alternative, chemicals testing strategy using a high definition toxicogenomics and zebrafish (Danio rerio) embryos. Toxicol. Sci. 118, 128–139.
Seabra, A.B., Paula, A.J., de Lima, R., Alves, O.L., Durán, N., 2014. Nanotoxicity of graphene and graphene oxide. Chem. Res. Toxicol. 27, 159–168.
Shaked, I., Zimmerman, G., Soreq, H., 2008. Stress-induced alternative splicing modulations in brain and periphery: acetylcholinesterase as a case study. Ann. N. Y. Acad. Sci. 1148, 269–281.
Shams, S., Chatterjee, D., Gerlai, R., 2015. Chronic social isolation affects thigmotaxis and whole-brain serotonin levels in adult zebrafish. Behav. Brain Res. 292, 283–287.
Shams, S., Seguin, D., Facciol, A., Chatterjee, D., Gerlai, R., 2017. Effect of social isolation on anxiety-related behaviors, cortisol, and monoamines in adult zebrafish. Behav. Neurosci. 131, 492.
Shaw, E., 1960. The development of schooling behavior in fishes. Physiol. Zool. 33, 79–86.
Smith, S.C., Ahmed, F., Gutierrez, K.M., Rodrigues, D.F., 2014. A comparative study of lysozyme adsorption with graphene, graphene oxide, and single-walled carbon nanotubes: potential environmental applications. Chem. Eng. J. 240, 147–154.
Souza, J.P., Baretta, J.F., Santos, F., Paino, I.M., Zucolotto, V., 2017. Toxicological effects of graphene oxide on adult zebrafish (Danio rerio). Aquat. Toxicol. 186, 11–18.
Souza, J.P., Venturini, F.P., Santos, F., Zucolotto, V., 2018. Chronic toxicity in Ceriodaphnia dubia induced by graphene oxide. Chemosphere 190, 218–224.
Stankovich, S., Dikin, D.A., Piner, R.D., Kohlhaas, K.A., Kleinhammes, A., Jia, Y., Wu, Y., Nguyen, S.T., Ruoff, R.S., 2007. Synthesis of graphene-based nanosheets via chemical reduction of exfoliated graphite oxide. Carbon 45, 1558–1565.
Steele, W.B., Kristofco, L.A., Corrales, J., Saari, G.N., Haddad, S.P., Gallagher, E.P., Kavanagh, T.J., Kostal, J., Zimmerman, J.B., Voutchkova-Kostal, A., 2018. Comparative behavioral toxicology with two common larval fish models: exploring relationships among modes of action and locomotor responses. Sci. Total Environ. 640, 1587–1600.
Tu, X., Li, Y.-W., Chen, Q.-L., Shen, Y.-J., Liu, Z.-H., 2020. Tributyltin enhanced anxiety of adult male zebrafish through elevating cortisol level and disruption in serotonin, dopamine and gamma-aminobutyric acid neurotransmitter pathways. Ecotoxicol. Environ. Saf. 203, 111014.
Volgin, A.D., Yakovlev, O.A., Demin, K.A., Alekseeva, P.A., Kalueff, A.V., 2019. Acute behavioral effects of deliriant hallucinogens atropine and scopolamine in adult zebrafish. Behav. Brain Res. 359, 274–280.
Wang, X., Zheng, Y., Zhang, Y., Li, J., Zhang, H., Wang, H., 2016. Effects of β-diketone antibiotic mixtures on behavior of zebrafish (Danio rerio). Chemosphere 144, 2195–2205.
Wei, L., Wu, F., Shi, D., Hu, C., Li, X., Yuan, W., Wang, J., Zhao, J., Geng, H., Wei, H., 2013. Spontaneous intercalation of long-chain alkyl ammonium into edge-selectively oxidized graphite to efficiently produce high-quality graphene. Sci. Rep. 3, 2636.
Wong, K., Elegante, M., Bartels, B., Elkhayat, S., Tien, D., Roy, S., Goodspeed, J., Suciu, C., Tan, J., Grimes, C., 2010. Analyzing habituation responses to novelty in zebrafish (Danio rerio). Behav. Brain Res. 208, 450–457.
Yang, X., Yang, Q., Zheng, G., Han, S., Zhao, F., Hu, Q., Fu, Z., 2019. Developmental neurotoxicity and immunotoxicity induced by graphene oxide in zebrafish embryos. Environ. Toxicol. 34, 415–423.
Yao, Y., Ren, L., Gao, S., Li, S., 2017. Histogram method for reliable thickness measurements of graphene films using atomic force microscopy (AFM). J. Mater. Sci. Technol. 33, 815–820.
Yusoff, A.R.M., 2014. Graphene Optoelectronics: Synthesis, Characterization, Properties, and Applications. Wiley.
Zhang, X., Zhou, Q., Zou, W., Hu, X., 2017. Molecular mechanisms of developmental toxicity induced by graphene oxide at predicted environmental concentrations. Environ. Sci. Technol. 51, 7861–7871.
Zhao, G., Li, J., Ren, X., Chen, C., Wang, X., 2011. Few-layered graphene oxide nanosheets as superior sorbents for heavy metal ion pollution management. Environ. Sci. Technol. 45, 10454–10462.